International Information and Engineering Technology Association
Advancing the World of Information and Engineering

International Journal of Heat and Technology
Vol. 40, No. 2, April, 2022, pp. 535-542
Journal homepage: http://iieta.org/journals/ijht

# Effect of Heat Input and Filling Ratio on Raise in Temperature of the Oscillating Heat Pipe with Different Working Fluids Using ANN Model

M. Prashanth[1], D. Madhu[2], K. Ramanarasimh[3], R Suresh[4*]

[1] Dept. of Mechanical Engineering, Government Engineering College, Hassan 573201, Karnataka, India
[2] Dept. of Mechanical Engineering, Government Engineering College, Ramanagara 562159, Karnataka, India
[3] Dept. of Mechanical Engineering, K.S School of Engineering and management, Banaglore 560109, India
[4] Dept. of Mechanical and Manuf. Engineering, M.S Ramaiah University of Applied Sciences, Bangalore 560058, India

Corresponding Author Email: suresh.me.et@msruas.ac.in

https://doi.org/10.18280/ijht.400221

**Received:** 16 March 2022
**Accepted:** 6 April 2022

***Keywords:***
*Oscillating Heat Pipe (OHP), acetone, ethanol, methanol, filling ratio, heat input, Artificial Neural Network (ANN)*

**ABSTRACT**

In the present article, feed forward multilayer perceptron neural network (FFMLPNN) model has been used to predict the rise in temperature in closed loop oscillating heat pipe filled with three different fluid i.e., Acetone, methanol and ethanol respectively. Experimental test was carried out for the inner diameter of 1.7mm copper tube for all the combinations of filling ratio, heat input and time taken to evaluate the performance of the OHP. Totally 2000 data sets have been used for Acetone and Methanol, 1500 data sets is used for ethanol in the present NN model. ANN model with FFMLPNN using three input parameter (Filling ratio, heat input and time taken) and rise in temperature has output parameter respectively. Levenberg-Marquardt algorithm with a 4-10 neurons has been used for the determination of optimal model. The 3-8-1 combinations predict the rise in temperature for ethanol and acetone whereas for methanol 3-7-1 is the optimal combinations was achieved. For all the combinations RMSE values are 0.3414, 0.1285 and 0.1237 (Training-70%), 0.3526, 0.1375, 0.1234 (testing-15%) and 0.3010, 0.1515, 0.1425 (validation-15%). The values for coefficient of determinations are 0.9941, 0.9975 and 0.9971 for methanol, acetone and ethanol was achieved. The results clearly indicated that the proposed MLPANN model can successfully predict the rise in temperature.

## 1. INTRODUCTION

In heat pipes, pulsating heat pipe was the promising device for the heat transportation in heat transfer unit. Therefore micro-grooved oscillating heat pipe (OHP) is one of the effective modes to evaluate the performance heat transfer of the system. This device would enhance the allowable input heat flux by condensate the backflow to the evaporator when the filling ratio ranging from 30% to 60% [1]. Due to increase in filling ratio, heat added to the evaporator section leads to increase in temperature and pressure during the flow process. Therefore filling ratio was the major part to increase the heat input for the oscillation motion of the working fluid [2]. To heat the oscillating pipe many methods was applied in the evaporator section. There was a pulsed supply with regulated current method was used to heat the system. This method generates a large amplitude oscillation to heat up for a short period of time [3]. Temperature distribution for the thermal management of the oscillating heat pipe with copper particles in the evaporator was investigated. At low filling ratio of 30% temperature distribution was good uniformity by neglecting the gravity action was achieved in this study [4]. In anti-gravity OHP system high temperature was exist in the exhaust to preheat. For this current 35 turns OHP with a filling ratio of 70% gave a better bond number from 0.814 to 0.986 for the same geometry it exhibits a better heat transfer [5].

The performance of the OHP using $Al_2O_3$ nano-particles with a particle size of 56nm by considering the filling ratio, mass fraction of the nano-particles and power inputs to determine the thermal resistance was carried out. For the mass fraction of 0.9% there was a decrease by 0.14°C/W was achieved compare to water filled OHP [6]. Different mathematical models were used to determine the internal motion of working fluid mechanism in the closed loop OHP. The simulation study shows that the heating period and heating interval factors are major concerned for the evaluation of the heat transfer enhancement in OHP [7]. Temperature distribution and heat transfer rate using iron oxide and kerosene as a nano fluid in copper OHP was studied. Addition of iron oxide gives a better performance with an increase in in heat transfer coefficient and difference temperature between the surface and the vapor was 3.1°C and 2°C respectively [8]. To increase the heat transfer mechanisms of oscillating pipe a mathematical model was developed by considering spring mass system to for an annular flow with a slug causing of penetrate liquid. This flow trains the liquid by disappearing the vapour bubbles by creating the pulsating effect of the liquid [9]. For the performance improvement of oscillating pipe mixing of self-rewetting fluids and nanofluids was developed. To determine the high performance of the OHP optimum concentration of the nanoparticles (16%) and self-rewetting (12%) was used [10].

In case of hybrid flexile oscillating heat pipe at the adiabatic section at the heating and cooling side, a micro grooved copper tube was designed and fabricated. This structural design creates a deformation of adiabatic section and exhibits a spatial flexibility to improve the heat transfer performance of the new design [11]. If the filling ratio was 40% to 80% in case of self-rewetting fluid can ensure a higher heating load compare to water or ethanol as a working medium with a filling ratio of 30% [12]. With the same combinations heat transfer coefficient was determined using iron oxide and kerosene as a nano fluids for a different inclination angle from 0° to 90° with 10 to 90W heat input. For the critical angle of 75° heat transfer coefficient was increase due to increase in inclination angle [13]. Temperature was measured between internal fluid and external wall to determine the temperature gradient using T-type thermocouple. Results revealed that the difference in temperature being smaller in the length wise of fluid columns compare to the wall due to strong advection effect in the OHP heat transfer [14]. Even effect of governing parameters also effect on the flow of nano-fluids in the OHP system and the optimization of the tube diameters also presented in this study [15]. In helical coiled OHP with a copper material using ethanol and methanol as a working fluid with a 60% volume filled ratio was carried out experimentally. The result shows that the heat flux was less than 70W for ethanol and 105W for methanol was achieved in the designed heat pipe [16].

Multilayer OHP was also employed for the measurement of heat transfer rate and it was effectively work for all the working fluids [17]. To determine the characteristics of the working fluids micro OHP was used with trapezoidal channels. Two different start-up behaviours were used and Comparison was made, it can be concluded that bubble nucleation at the start-up was better than that of without bubble nucleation [18]. To measure performance of the start-up mechanism filling ratio, heat input, working fluids are the major concern in evaluation process. Finally in case of acetone filled OHP had a higher thermal performance compare to the water filled OHP at 60 and 300W [19]. For the feasibility study radial basis function model was used to determine the heat transfer and also pressure drop for the water based with magnesium oxide nanoparticles. It's clearly shows that the predicted value heat transfer coefficient with 0.99% and 0.995% accuracy with an optimum value of $\varphi$=0.125% [20].

In case of heat exchangers for oscillating flow of thermo acoustic devices new ANN approach was used to determine the heat transfer coefficient. An optimum value was achieved for two input parameters with ten neurons at one output give a better performance of heat transfer coefficient [21]. Different methods such as machine learning approach were used to measure the heat transfer in the heat pipe. For the better performance of the complex problems of the heat pipes some of the potential methods was included in the research [22]. Apart from ANN method genetic algorithm with a multi-objectives optimization was used for the thermo-acoustic applications. For different parameters such as length of the stacks, center position of the stack and spacing of the plate. Optimum values were 4cm for length of the stack, 4cm center position and 0.36 cm for gap separation between the stacks was determined [23]. During the cutting of difficult materials, high heat will generate and its effects the thermal damage for both the tool and workpiece. ANN was used to predict the heat transfer coefficient during cutting process. The percentage error was 0.01% and 13.9% for training and testing was achieved [24]. To predict heat transfer for the roughened absorber plate using feed forward neural network was used. Levenberg-Marquardt algorithm with ten neurons for five input variables gives the satisfactory results [25]. It is due to the flow pattern change from slug/plug flow to annular flow, recent experimental and theoretical findings have indicated that the latter dominates the heat transfer mechanism in an OHP, especially at relatively high power inputs. Clearly, a low filling ratio (FR) is advantageous for the aforesaid flow pattern transition and the reduction in oscillating motion frictional resistance, which improves latent heat conduction. If the minimum temperature difference between the condenser and evaporator sections is assumed to be 10°C, and then the maximum uncertainty of the effective thermal conductivity is estimated to be minimum, if the heat dissipation is not considered [1-5].

Based on the about observations, different artificial neural network prediction methods were used for the measurement of heat transfer coefficient, thermal resistance and temperature between the condenser and evaporator in OHP. Comparative analysis by considering different input variables was not considered in the previous analysis. Hence in the present investigation three variables with one output variables (temperature rise) was considered for the different fluid conditions such as acetone, ethanol and methanol. Final results were compared for the optimum values for the minimum temperature rise was analysed.

## 2. EXPERIMENTAL METHOD

Experiments was conducted by using a fabricated four turned oscillating heat pipe setup consists of copper tubes, glass tube, silicon rubber tube, mica heater, condenser, K-type thermocouple, glass wool, data acquisition system, and heat control unit respectively. Acetone, ethanol and methanol was used to measure the temperature rise of the OHP system and there properties is shown in Table 1 and properties of working fluids is as in Table 1. To measure the temperature, filling ratio (50%, 60%, 70% and 80%), heat input (25 W, 30 W, 35 W and 40 W) was considered for all the combinations considered for acetone and methanol whereas, ethanol filling ratio (50%, 60%, 70% and 80%), heat input as (30 W, 35 W and 40 W) and time duration for the both the combinations considered as an input to the OHP.

**Table 1.** Properties of working fluids

| Fluids | Boiling Point (°C) | Melting Point (For Solid State) (°C) | Useful Temp. Range (°C) | Specific Heat $C_p$ (J/Kg K) |
|---|---|---|---|---|
| Acetone | 57 | -95 | 0-120 | 2031 |
| Methanol | 64.7 | -97.6 | 0-200 | 2531 |
| Ethanol | 78 | -112 | 0-130 | 2470 |

The procedure for conducting an experiment includes the initial check for any leakage in fluid circuit, connectivity and readout from thermocouples display in acquisition system. Subsequently, heat input to the mica heater plate is adjusted with a power controller to maintain the steady state temperature. The temperature reading for a particular heat input is recorded after the system reaches steady state. The heat sink ensures the heat removal at the copper pipes. The temperature is monitored through the data acquisition system. The experiment is repeated by varying the heating rates at the source and correspondingly at the sink. The overall oscillating heat pipe setup is shown in Figure 1. For acetone and methanol the heat input range considered were 25W, 30W, 35W and

40W. Heat input for ethanol were 30W, 35W and 40W. The reason for choosing different heating rates is, no fluctuation in temperature was observed between 25W to 30W. Therefore the change in temperature was shown from 30W onwards in the experimentation.

## 3. RESULTS AND DISCUSSION

Temperature rise of the OHP using acetone, ethanol and methanol was determined by considering filling ratio of 50%, 60%, 70%, 80% and heat input of 25W, 30W, 35W and 40W (acetone and methanol) and for ethanol heat input was considered as 30W, 35W and 40W respectively. The difference in temperature of evaporator and condenser section temperatures with heat input is studied at steady state condition. The results were drawn based on the experimentation and the same data was used for the ANN model for the analysis. For the present analysis 2000 data sets was used for the obtained results indicated that higher filling ratio of working fluid shows the better results in terms of reduction in difference in temperature, increased heat transfer coefficient across the evaporator and condenser. Finally experimental result was validated by using ANN models. Based on uncertainty analysis, measured and predicted values were explained in details for the better understanding of the developed OHP.

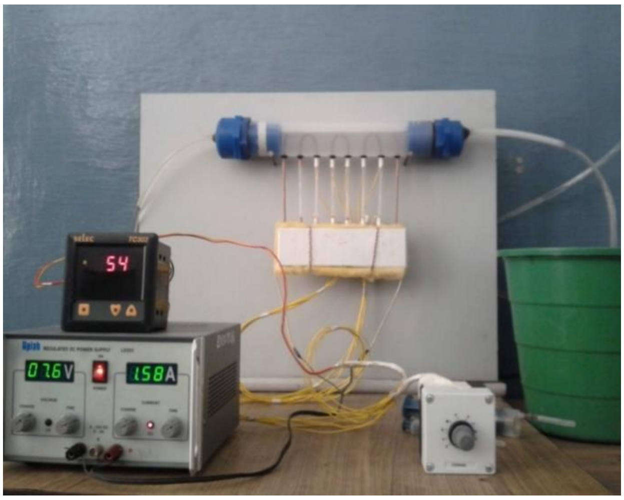

**Figure 1.** Oscillating heat pipe experimental setup

### 3.1 Effect of heat input on temperature rise with different fluids

For all the filling ratio of 50% to 80% by varying the heat input of 25 W to 40 W for acetone and methanol, heat input of 30W to 40W for ethanol was noted down. The oscillations of temperature within the copper tube were determined. Oscillations depends on the thermal properties of the filled fluid and the heat input. At the heat input of 25 W to 40 W in for acetone and methanol 258 seconds was considered for all the combinations, whereas in case of ethanol 30 W, 35 W and 40W with a filling ration of 50% to 80% 248s was considered. At the filling ratio of 50% to 80% with 25W to 40W heat input the temperature varies from 41.5°C to 38.25°C and 36.5°C to 34.25°C for acetone and methanol, whereas, in ethanol filling ratio from 50% to 80% with 30 W to 40 W heat input temperature varies from 59.25°C to 62°C respectively. Therefore there was an minimum temperature different was measured for 80% filling ratio at 40 W heat input. The effect of heat input on average temperature rise (Te-Tc) with different filling ratio for acetone, methanol and ethanol is as in Figure 2.

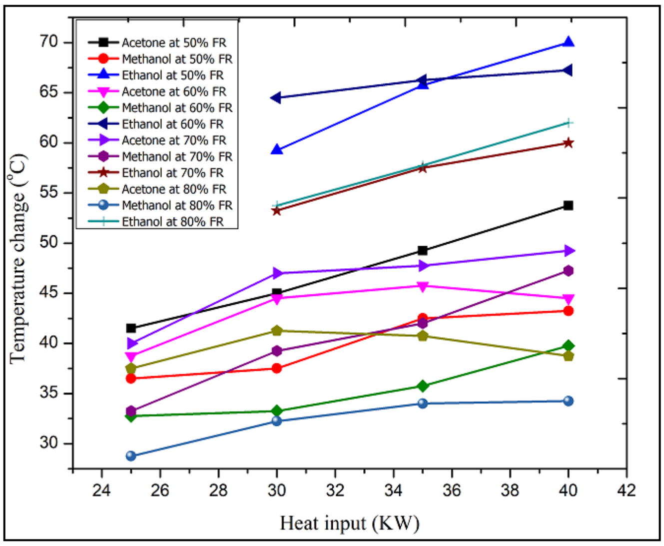


**Figure 2.** Effect of heat input on average temperature rise (Te-Tc) with different filling ratio for acetone, methanol and ethanol

The proposed work used an MLPNN model is a feed forward-backward propagation artificial neural network to predict the temperature rise in the OHP for all the combinations considered. The structure of the model is developed in three different layers. By adjusting the weights of individual input parameters to the hidden layer Levenberg-Marquardt (LM) algorithm was used by considering the different neurons to predict the output parameter. To minimize the mean square error LM algorithm with FFBPNN is used. For this algorithm different transfer function can be used for the better fit between the variables based on the trial and error method.

In training process, the input parameters enters the FFNN is shown in Figure 3. Each product of input parameters (Mi) and a weight function (Wij) are summed into the junction and is summed with bias (bj) of the neurons as in Eq. (1). In the present investigation, the input variables such as filling ratio, time taken and heat input were used and the output parameter is the temperature rise is considered.

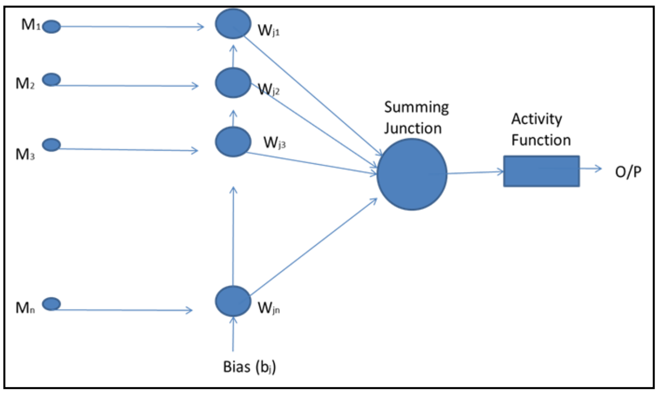


**Figure 3.** Generalized structure of artificial neurons

$$X = \left(\sum_{i=1}^{n} (W_{ij} M_i)\right) + b_j \quad (1)$$

During the training and testing period the input and target data which enters into the network. The input data is trained by using learning algorithms. The most commonly used algorithm is Levenberg-Marquardt (LM) is faster than other learning algorithms. For artificial neural network analysis, Mat lab software was used. The widely used activity function is tanh function with values ranges from -1 to +1 is as in Eq. (2) and is written as:

$$F(X) = \frac{e^x - e^{-x}}{e^x + e^{-x}} \quad (2)$$

### 3.2 ANN models developed for temperature rise in OHP for acetone, ethanol and methanol

In the present models, totally 2000 data sets for acetone and methanol, 1500 data sets for ethanol were used to develop models. The proposed MLPNN model is used to predict the temperature rise of all the combinations considered is shown in Figure 4. In the input layer, three input parameters were used such as filling ratio, time taken and heat input, the temperature rise has been taken at the output layer.

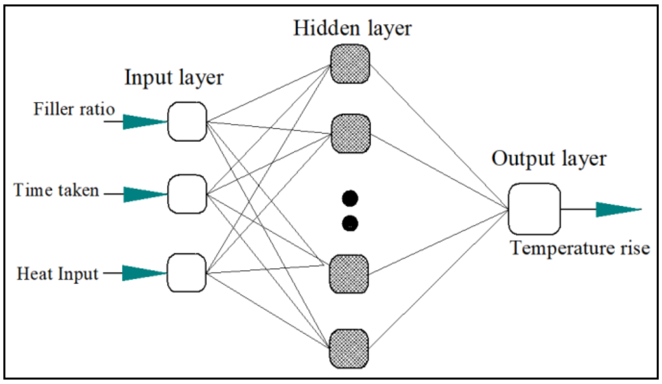


**Figure 4.** ANN model for three inputs with one output parameter

**Table 2.** Weight and bias values for acetone at 3-7-1 performance results

| Weights between the input and hidden layer ($W_{7*3}$) | Weights to output layer ($W_{7*1}$) |
|---|---|
| 1.2331 | 8.4616 |
| -0.88975, -2.4521, 0.14024; | 1.3635 |
| -0.45611, -8.3633, -1.4089; | 0.24642 |
| 1.3607, -6.8306, 0.11702; | -3.0516 |
| -2.3418, 9.7768, 0.05502; | -1.7102 |
| 0.7368, 0.17938, 0.30956; | 0.05025 |
| -0.63829, -0.62903, 0.063767 | -1.4921 |
| **Bias in hidden layer ($B_{1*7}$)** | **Bias in output (B1*1)** |
| -1.6298; 2.3221; -1.0223; -0.60998; -0.67028; 1.6873; 3.6424 1.2331 | 2.23 |

For acetone and methanol in 2000 data sets for each type of filling fluids, training consists of 1400 data sets whereas testing and validation consists of 300 data sets each. For ethanol in 1500 data sets for each type of filling ratio training consists of 1050 data sets whereas testing and validation consists of 225 data sets. Feed forward back propagation learning algorithm was applied for the present models. In this study LM back propagation algorithm was used for the training, testing and validation process. The trial and error method for the hidden layer was used to set the number of neurons before the weight functions of the input is considered. Using this technique, 4-10 neurons have been used with the single hidden layer. Tansig transfer function as a sigmoid function for the hidden layer was considered (Table 2, Table 3 and Table 4). The detailed optimum values for MSE of acetone, ethanol and methanol shows in Figures 5, 6 and 7 respectively. Similarly the $\boldsymbol{R^2}$ for training, testing and validation are shown Figures 8, 9 and 10 respectively.

**Table 3.** Weight and bias values for ethanol at 3-7-1 performance results

| Weights between the input and hidden layer ($W_{7*3}$) | Weights to output layer ($W_{7*1}$) |
|---|---|
| -2.8114, -5.4684, 0.57911; | 1.3967 |
| -5.1018, -6.4354, 0.93094; | 2.3902 |
| -1.2805, -1.3569, -0.99675; | -1.1175 |
| 6.9133, 8.0273, 2.2808; | -0.055317 |
| 6.2072, -2.926, 0.76667; | 7.4785 |
| -0.11764, 0.25041, -0.48527; | 0.81309 |
| 1.068, 1.3691, -0.18972; | 2.4272 |
| **Bias in hidden layer ($B_{1*7}$)** | **Bias in output (B1*1)** |
| 4.7406; 3.8968; 0.75421; -0.46686; 3.6221; -3.7781; 1.4843 | -2.1574 |

**Table 4.** Weight and bias values for methanol at 3-8-1 performance results

| Weights between the input and hidden layer ($W_{8*3}$) | Weights to output layer ($W_{8*1}$) |
|---|---|
| 38.1868, 25.2111, 1.7168; | 11.7388 |
| 13.4225, 2.9127, 0.28645; | -15.3289 |
| 0.40287, -0.02495, 0.00520; | -0.21043 |
| -0.17229, 0.00830, -0.00365; | 0.29484 |
| 7.6552, 32.0678, 1.45100; | 26.6871 |
| 25.8291, -1.7968, -0.03214 | 24.0228 |
| 13.5412, -1.8541, -0.08759 | 11.7388 |
| **Bias in hidden layer ($B_{1*7}$)** | **Bias in output (B1*1)** |
| 4.7406; 3.8968; 0.75421; -0.46686; 3.6221; -3.7781; 1.4843 | 6.2038 |

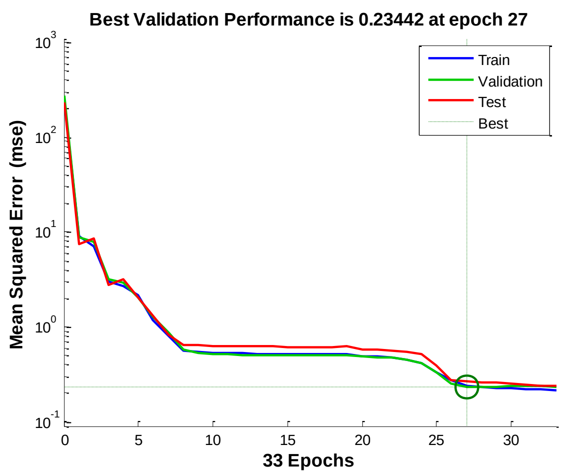


**Figure 5.** Optimum value for MSE of acetone for seven neurons

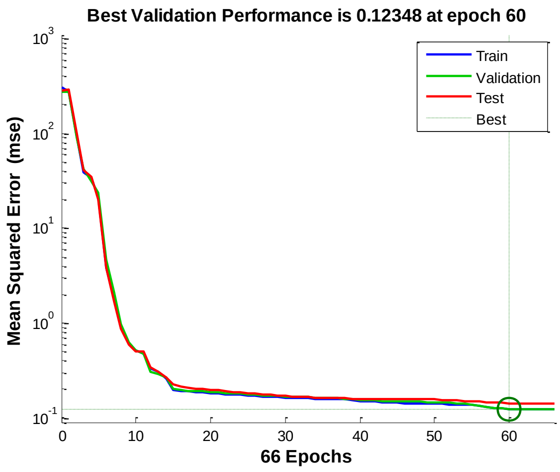


**Figure 6.** Optimum value for MSE of ethanol for seven neurons

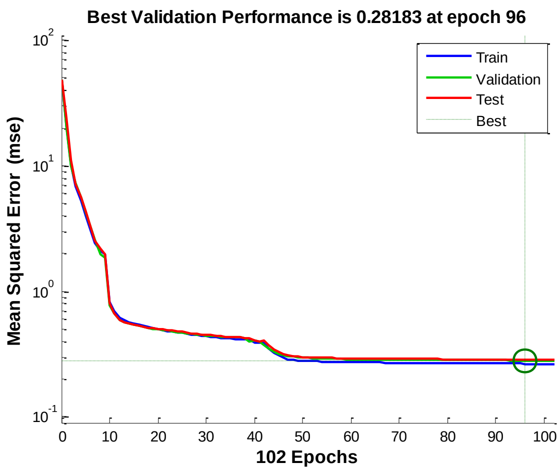


**Figure 7.** Optimum value for MSE of methanol for eight neurons

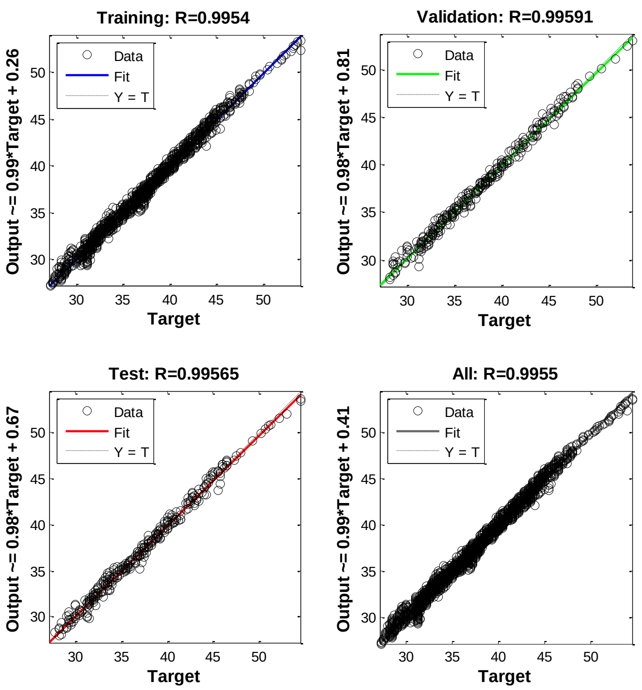


**Figure 8.** Regression analysis for training, testing and validation for acetone

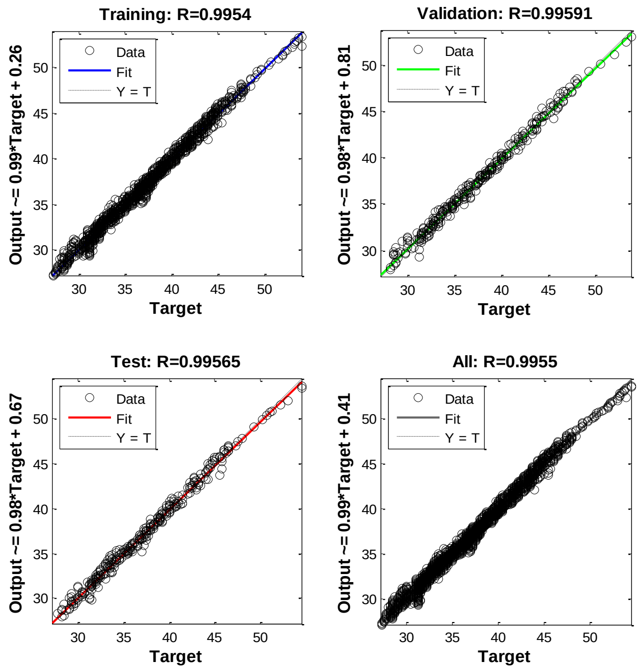


**Figure 9.** Regression analysis for training, testing and validation for ethanol

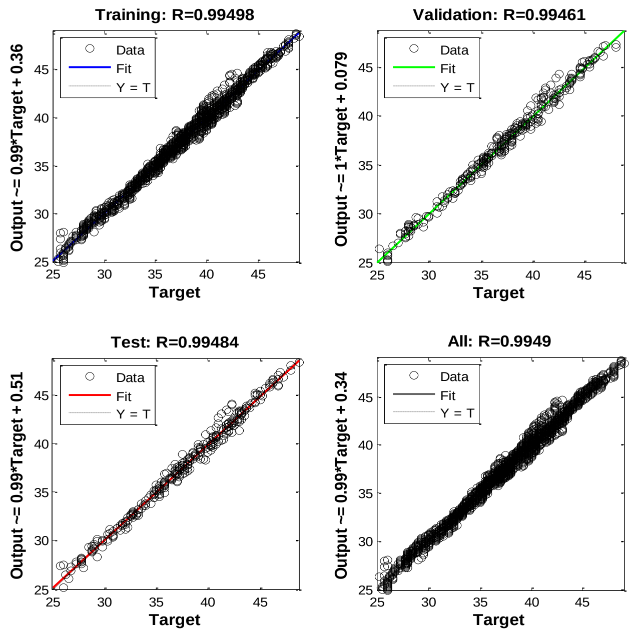


**Figure 10.** Regression analysis for training, testing and validation for methanol

### 3.3 Performance prediction models

To evaluate the correlation coefficient between the measured values to the predicted values performance prediction is the good indicator to derive the model. To define the performance predictions VAF, RMSE and MAPE are the predictive capacity of the models was evaluated. Figures 11, 12 and 13 shows the error values for acetone, ethanol and methanol for all the combinations of filling ratio, heat input and time taken. The following equations show the performance predictive is shown in Eq. (3), (4), (5) respectively. Training, testing and validation performance for OHP with methanol, ethanol and acetone are in Table 5-7. ANN Predicted $\boldsymbol{R^2}$ values for acetone, ethanol and methanol of these models during training stage is 0.9945, 0.9975, and 0.9941 respectively. During testing stage $R^2$ is 0.9972, 0.9969, and 0.9932 and for validation $R^2$ is 0.9972, 0.9968, and 0.9986 respectively.

$$\mathrm{VAF} = 1 - \frac{var(y - y')}{var(y)} \times 100 \tag{3}$$

$$RMSE = \sqrt{\frac{1}{\mathrm{N}}\sum_{\mathrm{i}=1}^{\mathrm{N}}(\mathrm{y} - \mathrm{y}')^2} \tag{4}$$

$$MAPE = \frac{1}{N}\sum_{i=1}^{N}\left|\frac{Ai - Pi}{Ai}\right| \times 100 \tag{5}$$

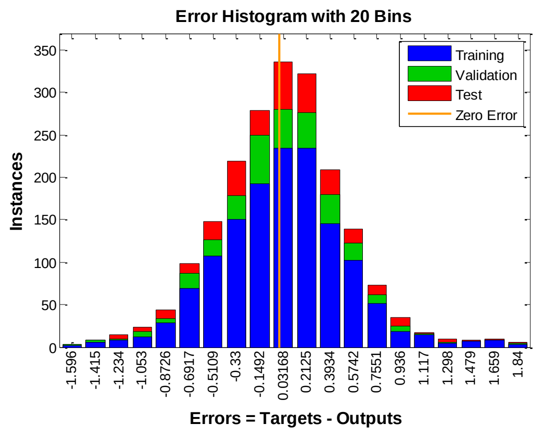


**Figure 11.** Error values for acetone for all the combinations of filler ratio, heat input and time taken

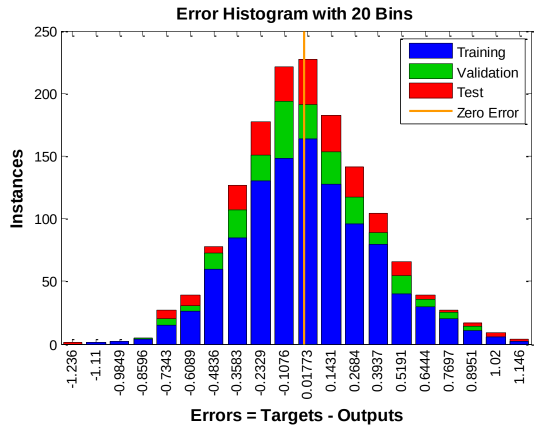


**Figure 12.** Error values for ethanol for all the combinations of filling ratio, heat input and time taken

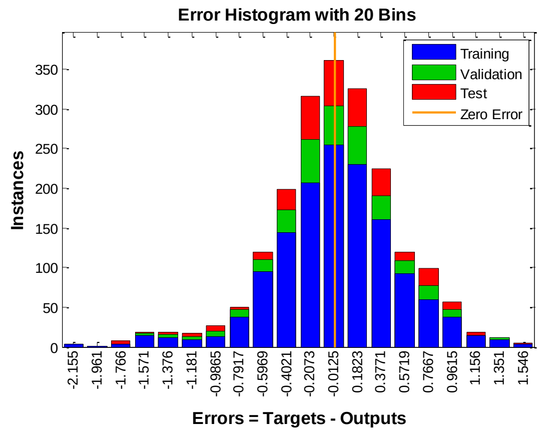


**Figure 13.** Error values for methanol for all the combinations of filling ratio, heat input and time taken

**Table 5.** Training, testing and validation performance for OHP with methanol

| No. of Neurons | Training | | Testing | | Validation | |
|---|---|---|---|---|---|---|
| | RMSE | $R^2$ | RMSE | $R^2$ | RMSE | $R^2$ |
| 4 | 1.3883 | 0.9737 | 1.2496 | 0.9734 | 1.4058 | 0.9752 |
| 5 | 1.3740 | 0.9745 | 1.2148 | 0.9789 | 1.2612 | 0.9804 |
| 6 | 0.8425 | 0.9854 | 0.7421 | 0.9871 | 0.8122 | 0.9891 |
| 7 | 0.3719 | 0.9930 | 0.3821 | 0.9924 | 0.3079 | 0.9942 |
| 8 | 0.3414 | 0.9941 | 0.3526 | 0.9932 | 0.3010 | 0.9986 |
| 9 | 0.4161 | 0.9821 | 0.4615 | 0.9844 | 0.3912 | 0.9812 |
| 10 | 0.4264 | 0.9811 | 0.4832 | 0.9802 | 0.4121 | 0.9804 |

**Table 6.** Training, testing and validation performance for OHP with acetone

| No. of Neurons | Training | | Testing | | Validation | |
|---|---|---|---|---|---|---|
| | RMSE | R2 | RMSE | $R^2$ | RMSE | $R^2$ |
| 4 | 0.7317 | 0.9861 | 0.7276 | 0.9863 | 0.6272 | 0.9884 |
| 5 | 0.3838 | 0.9927 | 0.4129 | 0.9922 | 0.4241 | 0.9823 |
| 6 | 0.3528 | 0.9934 | 0.3123 | 0.9941 | 0.3752 | 0.9925 |
| 7 | 0.1285 | 0.9975 | 0.1375 | 0.9973 | 0.1515 | 0.9972 |
| 8 | 0.2359 | 0.9953 | 0.2344 | 0.9959 | 0.2663 | 0.9956 |
| 9 | 0.1442 | 0.9891 | 0.1462 | 0.9846 | 0.1632 | 0.9811 |
| 10 | 0.1529 | 0.9822 | 0.1633 | 0.9822 | 0.1648 | 0.9802 |

**Table 7.** Training, testing and validation performance for OHP with ethanol

| No. of Neurons | Training | | Testing | | Validation | |
|---|---|---|---|---|---|---|
| | RMSE | $R^2$ | RMSE | $R^2$ | RMSE | $R^2$ |
| 4 | 0.4246 | 0.9906 | 0.4118 | 0.9903 | 0.3343 | 0.9926 |
| 5 | 0.2184 | 0.9950 | 0.2360 | 0.9941 | 0.2274 | 0.9948 |
| 6 | 0.1656 | 0.9962 | 0.1751 | 0.9955 | 0.1958 | 0.9959 |
| 7 | 0.1093 | 0.9975 | 0.1331 | 0.9969 | 0.1216 | 0.9968 |
| 8 | 0.1237 | 0.9971 | 0.1234 | 0.9970 | 0.1425 | 0.9967 |
| 9 | 0.1164 | 0.9914 | 0.1841 | 0.9902 | 0.1487 | 0.9914 |
| 10 | 0.1322 | 0.9908 | 0.1862 | 0.9894 | 0.1566 | 0.9863 |

## 4. CONCLUSIONS

A new modelling approach for the oscillating heat pipe based on artificial neural network technique had been presented in this work. A three layered FFBPNN with a configuration of three inputs with one output was adopted in the present paper. For all the three different forms of filling ratio of acetone, ethanol and methanol 4 to 10 neurons were selected to perform the models. For all the combinations temperature rise was analysed to evaluate the performance of the OHP. In this models LM algorithm with tansig transfer function was used to determine the performance indices such as VAF, RMSE and MAPE. For different filling ratio, heat input and time taken minimum RMSE was achieved for acetone of 0.1285, ethanol of 0.1093 and methanol of 0.3414 with a coefficient of determination of 0.9975, 0.9974, and 0.9941 respectively. Therefore the developed models with tansig transfer function for LM algorithm predict the temperature rise in the OHP for the different filling ratio, heat input and time taken.

## ACKNOWLEDGMENT

The Authors thanks to Government Engineering College, Ramanagara, Karnataka, India, for the providing facilities to conduct the research work.

## REFERENCES

[1] Qu, J., Gyan, F., Lv, Y., Wang, Y. (2021). Experimental study on the heat transport capability of micro-grooved oscillating heat pipe. Case Studies in Thermal Engineering, 26: 101210. https://doi.org/10.1016/j.csite.2021.101210

[2] Yin, D., Rajab, H., Ma, H.B. (2014). Theoretical analysis of maximum filling ratio in an oscillating heat pipe. International Journal of Heat and Mass Transfer, 74: 353-357. https://doi.org/10.1016/j.ijheatmasstransfer.2014.03.018

[3] Xian, H., Xu, W., Zhang, Y., Du, X., Yang, Y. (2014). Thermal characteristics and flow patterns of oscillating heat pipe with pulse heating. International Journal of Heat and Mass Transfer, 79: 332-341. https://doi.org/10.1016/j.ijheatmasstransfer.2014.08.002

[4] Wang, H., Qu, J., Peng, Y., Sun, Q. (2019). Heat transfer performance of a novel tubular oscillating heat pipe with sintered copper particles inside flat-plate evaporator and high-power LED heat sink application. Energy Conversion and Management, 189: 215-222. https://doi.org/10.1016/j.enconman.2019.03.093

[5] Liu, X., Han, X., Wang, Z., Hao, G., Zhang, Z., Chen, Y. (2020). Application of an anti-gravity oscillating heat pipe on enhancement of waste heat recovery. Energy Conservation and Management, 205: 112404. https://doi.org/10.1016/j.enconman.2019.112404

[6] Qu, J., Wu, H., Cheng, P. (2010). Thermal performance of an oscillating heat pipe with $Al_2O_3$ water nano fluids. International Communications in Heat and Mass Transfer, 37(2): 111-115. https://doi.org/10.1016/j.icheatmasstransfer.2009.10.001

[7] Zhao, J., Wu, C., Rao, Z. (2020). Numerical study on heat transfer enhancement of closed loop oscillating heat pipe through active incentive method. International Communications in Heat and Mass Transfer, 115: 104612. https://doi.org/10.1016/j.icheatmasstransfer.2020.104612

[8] Goshayeshi, H.R., Goodarzi, M., Dahari, M. (2015). Effect of magnetic field on the heat transfer rate of kerosene/$Fe_2O_3$ nano fluid in a copper oscillating heat pipe. Experimental Thermal and Fluid Science, 68: 663-668. https://doi.org/10.1016/j.expthermflusci.2015.07.014

[9] Yin, D., Wang, H., Ma, H.B., Ji, Y.L. (2016). Operation limitation of an oscillating heat pipe. International Journal of Heat and Mass Transfer, 94: 366-372. https://doi.org/10.1016/j.ijheatmasstransfer.2015.11.039

[10] Su, X., Zhang, M., Han, X., Guo, X. (2016). Experimental study on the heat transfer performance of an oscillating heat pipe with self-rewetting nano fluid. International Journal of Heat and Mass Transfer, 100: 378-385. https://doi.org/10.1016/j.ijheatmasstransfer.2016.04.094

[11] Qu, J., Li, X., Cui, Y., Wang, Q. (2017). Design and experimental study on a hybrid flexible oscillating heat pipe. International Journal of Heat and Mass Transfer, 107: 640-645. https://doi.org/10.1016/j.ijheatmasstransfer.2016.11.076

[12] Zhao, J., Qu, J., Rao, Z. (2017). Experiment investigation on thermal performance of a large-scale oscillating heat pipe with self-rewetting fluid used for thermal energy storage. International Journal of Heat and Mass Transfer, 108: 760-769. https://doi.org/10.1016/j.ijheatmasstransfer.2016.12.093

[13] Goshayeshi, H.R., Goodarzi, M., Safaei, M.R., Dahari, M. (2016). Experimental study on the effect of inclination angle on heat transfer enhancement of a ferro-fluid in a closed loop oscillating heat pipe under magnetic field. Experimental Thermal and Fluid Science, 74: 265-270. https://doi.org/10.1016/j.expthermflusci.2016.01.003

[14] Gabriel Monroe, J., Aspin, Z.S., Fairley, J.D., Thompson, S.M. (2017). Analysis and comparison of internal and external temperature measurements of a tubular oscillating heat pipe. Experimental Thermal and Fluid Science, 84: 165-178. https://doi.org/10.1016/j.expthermflusci.2017.01.020

[15] Su, Y., Davidson, J.H., Kulacki, F.A. (2012). Numerical investigation of fluid flow and heat transfer of oscillating pipe flows. Experimental Thermal and Fluid Science, 54: 199-208. https://doi.org/10.1016/j.ijthermalsci.2011.11.021

[16] Yeboah, S.K., Darkwa, J. (2018). Thermal performance of a novel helically coiled oscillating heat pipe (HCOHP) for isothermal adsorption. An experimental study. Experimental Thermal and Fluid Science, 128: 49-58. https://doi.org/10.1016/j.ijthermalsci.2018.02.014

[17] Ibrahim, O.T., Monroe, J.G., Thompson, S.M., Shamsaei, N., Bilheux, H., Elwany, A., Bian, L. (2017). An investigation of a multi-layered oscillating heat pipe additively manufactured from Ti-6Al-4V powder. International Journal of Heat and Mass Transfer, 108: 1036-1047. https://doi.org/10.1016/j.ijheatmasstransfer.2016.12.063

[18] Sun, Q., Qu, J., Yuan, J., Wang, H. (2018). Start-up

characteristics of MEMS-based micro oscillating heat pipe with and without bubble nucleation. International Journal of Heat and Mass Transfer, 122: 15-528. https://doi.org/10.1016/j.ijheatmasstransfer.2018.02.003

[19] Hao, T., Ma, H., Ma, X. (2019). Heat transfer performance of polytetrafluoroethylene oscillating heat pipe with water, ethanol, and acetone as working fluids. International Journal of Heat and Mass Transfer, 131: 109-120. https://doi.org/10.1016/j.ijheatmasstransfer.2018.08.133

[20] Esfe, M.H., Kamyab, M.H., Alirezaie, A., Toghraie, D. (2021). Using radial basis function network to model the heat transfer and pressure drop of water based nanofluids containing MgO nanoparticles. Case Studies in thermal Engineering, 28: 101475. https://doi.org/10.1016/j.csite.2021.101475

[21] Rahman, A.A., Zhang, X. (2018). Prediction of oscillatory heat transfer coefficient for a thermoacoustic heat exchanger through artificial neural network technique. International Journal of Heat and Mass Transfer, 124: 1088-1096. https://doi.org/10.1016/j.ijheatmasstransfer.2018.04.035

[22] Wang, Z., Zhao, X., Han, Z., Luo, L., Xiang, J., Zheng, S., Liu, M., Yu, M., Cui, Y., Shittu, S., Hu, M. (2018). Advanced big-data/machine-learning techniques for optimization and performance enhancement of the heat pipe technology – A review and prospective study. Applied Energy, 294: 116969. https://doi.org/10.1016/j.apenergy.2021.116969

[23] Zolpakar, N.A., Mohd-Ghazali, N., Ahmad, R. (2016). Experimental investigations of the performance of a standing wave thermoacoustic refrigerator based on multi-objective genetic algorithm optimized parameters. Applied Thermal Engineering, 100: 296-303. https://doi.org/10.1016/j.applthermaleng.2016.02.028

[24] Qian, N., Wang, X., Fu, Y., Zhao, Z., Xu, J., Chen, J. (2020). Predicting heat transfer of oscillating heat pipes for machining processes based on extreme gradient boosting algorithm. Applied Thermal Engineering, 164: 114521. https://doi.org/10.1016/j.applthermaleng.2019.114521

[25] Ghritlahre, H.K., Prasad, R.K. (2018). Prediction of heat transfer of two different types of roughened solar air heater using Artificial Neural Network technique. Thermal Science and Engineering Progress, 8: 145-153. https://doi.org/10.1016/j.tsep.2018.08.014